Multicusp ion source with external rf antenna for production of protons

S. K. Hahto,[a] S. T. Hahto, Q. Ji, K. N. Leung, and S. Wilde
Lawrence Berkeley National Laboratory, 1 Cyclotron Road, Berkeley, California 94720

E. L. Foley and L. R. Grisham
Plasma Physics Laboratory, Princeton University, Princeton, New Jersey 08543

F. M. Levinton
Nova Photonics, Inc., Princeton, New Jersey 08540

(Received 3 September 2003; accepted 26 October 2003)

Proton beams are needed in neutral-beam injection for diagnostic development of an internal magnetic field measurement. High proton fraction, low axial energy spread, current density in excess of 30 mA/cm^2, and a parallel ion beam with cw operation are the requirements for the ion source/extraction system. A multicusp-type ion source with an external rf antenna was constructed at Lawrence Berkeley National Laboratory. A proton fraction of 85% and proton current density of 32 mA/cm^2 were achieved at 1.8 kW of rf power. Plasma parameters were measured with a rf compensated Langmuir probe. © *2004 American Institute of Physics.* [DOI: 10.1063/1.1642744]

I. INTRODUCTION

Multicusp-type ion sources are widely used to form positive ions. The source offers a large, uniform plasma with a magnetic-field-free region in the center. Traditionally, the plasma is created either by filament discharge[1] or by a rf antenna placed inside the ion source chamber.[2] Both of these configurations have suffered the drawback of short operating lifetimes. The external antenna source described in this article is expected to demonstrate a much longer operating lifetime, and fewer problems with arcing and impurities. This source was designed for use in the motional Stark effect with laser-induced fluorescence (MSE-LIF) diagnostic. This diagnostic is expected to enable the measurement of magnetic field magnitude and pitch angle in hot plasmas, with fields as low as 0.1 T.[3] In MSE-LIF it is essential that the ion-beam (IB) axial energy spread is as low as possible, and that the proton fraction of the extracted hydrogen IB is maximized. The IB should also be parallel when entering the neutralizer cell. Extracted current densities should be optimized to reach high perveance with the existing electrode geometry at a beam energy of 35–40 keV used in the diagnostic beam line at Princeton Plasma Physics Laboratory (PPPL). A multicusp-type ion source with an external rf antenna and a magnetic filter was constructed and tested at Lawrence Berkeley National Laboratory (LBNL) before delivery to PPPL. The compact source design means that rf powers below 2 kW produce an intense cw IB. The external antenna geometry removes all parts that are susceptible to damage from inside the plasma chamber, and thus should give a long service interval and lifetime for the ion source.

A. Preliminary tests

A source was constructed for initial testing of the external antenna operation. A quartz tube 20 mm in length and 75 mm in diameter was used as a plasma chamber. A copper tube was wrapped around the quartz to form the rf antenna. Figure 1 shows a schematic of the test source: The test source was operated with 13.56 MHz rf frequency and up to 2 kW of rf power. The extracted hydrogen spectrum is shown in Fig. 2. The proton fraction of the extracted hydrogen ions was 75%. The proton fraction of the total current, including impurities such as H_2O, was 50%. Figure 3 shows the extracted total ion current density as a function of rf power. From Fig. 3, it can be seen that a total current density of 80 mA/cm^2 was extracted from the test source at 1800 W of rf power. This corresponds to 40 mA/cm^2 proton current density. Based on the preliminary tests, a multicusp-type ion source with an external rf antenna and a magnetic filter field inside the plasma chamber was designed. A target of 30 mA/cm^2 of proton current density and 80% proton fraction was set for the multicusp source.

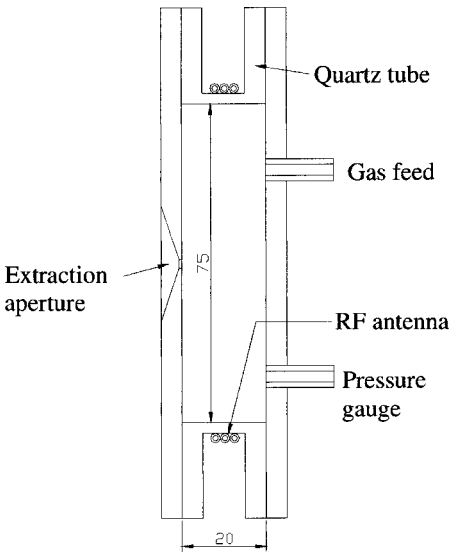

FIG. 1. A schematic of the external antenna test source.

[a]Electronic mail: skhahto@lbl.gov

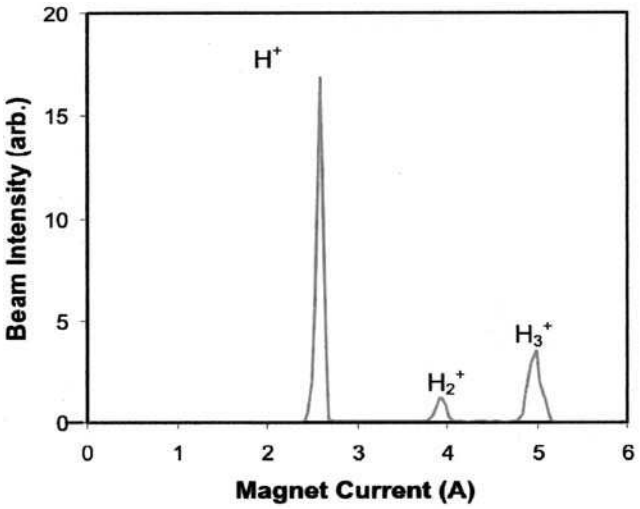

FIG. 2. Extracted hydrogen ion spectrum at 1.8 kW rf power. Impurities are not shown.

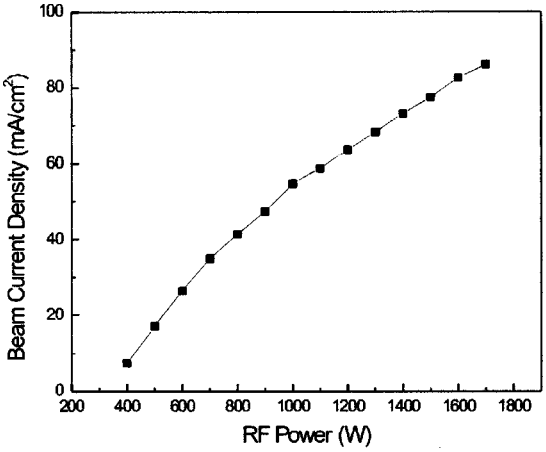

FIG. 3. Extracted total ion current as a function of the rf power.

B. External rf antenna multicusp source

A schematic of the constructed multicusp ion source is presented in Fig. 4. The source chamber is 87 mm long and consists of three separate parts. A quartz cylinder with 60 mm inner diameter is sandwiched between two copper chambers, each with 75 mm inner diameter. The rf antenna is a 2.5-turn, water-cooled copper tube wrapped around the quartz cylinder. The multicusp magnetic field confining the plasma is created with 14 SmCo magnet rows that are installed into both copper chambers. Two magnets are also installed in the back plate to complete the cusp lines in the back of the source and to prevent the flow of plasma to the laser input port extending from the back plate. Both chambers and end plates have water cooling to effectively remove heat in cw operation. In front of the extraction aperture, two smaller SmCo magnet bars are installed to create a transverse filter magnetic field. The filter is needed in order to have a uniform axial plasma potential distribution in the discharge region of the ion source, where most of the ionization takes place in the presence of the filter field. This minimizes the axial energy spread of the extracted ions and improves the proton fraction in the beam.[4,5] The 13.56 MHz rf generator and the accompanying inductive matching network are operated at the ion source potential, and the ion source is fully shielded to prevent the coupling of the rf into the extraction electrodes, which has been observed to increase the axial energy spread of the extracted IB.[6] The measured transverse filter magnetic field along the ion source center axis is plotted in Fig. 5. It has a maximum value of 90 G and full width at half-maximum of 16 mm.

II. EXTRACTION SIMULATIONS

The extraction system was designed to provide a parallel beam with 35 mA proton current and 35 keV beam energy at

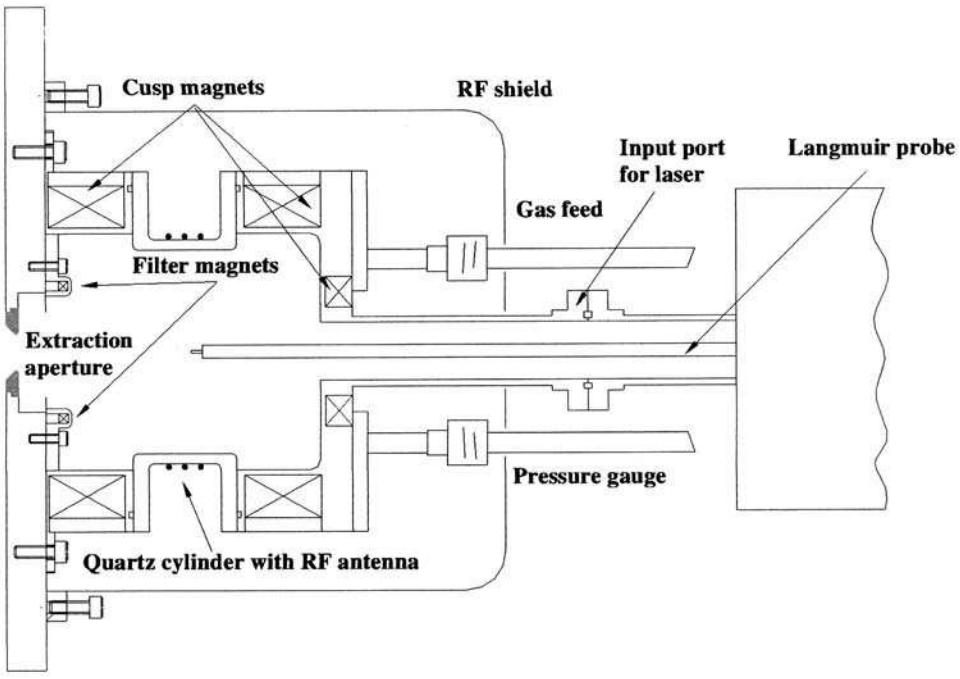

FIG. 4. The 75-mm-diameter, 87-mm-long multicusp source with an external rf antenna.

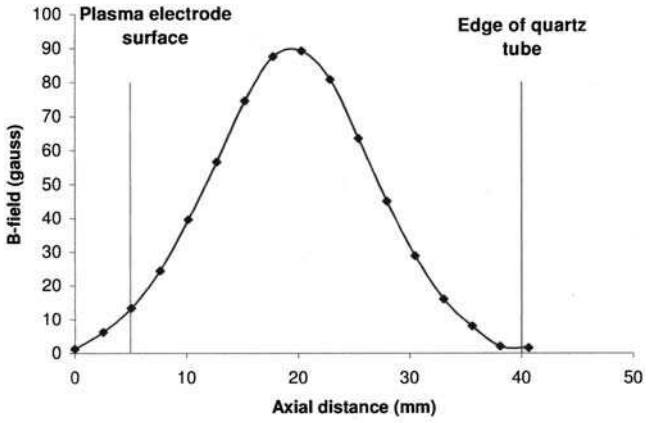

FIG. 5. The filter magnetic field measured along the center axis of the ion source.

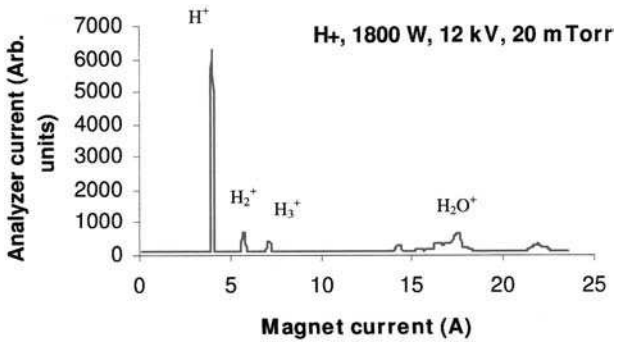

FIG. 7. Measured hydrogen mass spectrum at 1800 W of rf power, 12 kV extraction voltage, and 20 mTorr source pressure.

19 cm downstream from the extraction aperture. An existing three-electrode extraction system at PPPL was utilized. PBGUNS ion optical simulation code[7] was used in the simulations. Figure 6 show the PBGUNS simulation of the optimized extraction geometry with 99% beam space-charge neutralization starting from the ground electrode.

III. ION CURRENT AND SPECIES MEASUREMENTS

The ion source performance was characterized by measuring the IB mass spectrum, total IB current, and the axial plasma parameters. The ion source was installed in a test stand equipped with a 500 l/s turbomolecular pump. The total ion current was measured with a movable, secondary-electron-suppressed Faraday cup. When the IB mass spectrum was measured, the Faraday cup was retracted and the IB was focused into a magnetic-deflection mass spectrometer with an electrostatic einzel lens. The measurement setup used in the tests at LBNL was the same system that was used on a previous multicusp ion source experiment.[8] The beam was extracted from a 2 mm extraction aperture with an extraction gap of 4.5 mm. Figure 7 shows a typical hydrogen ion spectrum measured at 1800 W of rf power, 12 kV of extraction voltage, and 20 mTorr source pressure. About 85% of the positive hydrogen ions were H^+, 10% H_2^+, and 5% H_3^+. Some impurities can be seen in the spectrum; mainly water. The proton fraction was more than 70% if impurities were included in the species calculation. The level of impurities went down when the source was operated for a few hours. The source will have a larger extraction aperture when it is installed at PPPL, which should speed up the cleanup of the source due to the greater gas flow through the plasma chamber.

Figure 8 shows the measured total ion current at two different rf powers as a function of the extraction voltage. As can be seen, the ion current saturated at ~4 kV extraction voltage. Figure 9 shows the total ion and proton current densities as a function of rf power at 20 mTorr source pressure. The fraction of protons was determined from the mass spectra for each rf power.

From Fig. 9, it can be seen that a proton current density of 32 mA/cm^2 was achieved at 1800 W of rf power. This fulfills the proton current requirement set for the source.

Figure 10 shows the measured ion species fractions as a function of rf power. The proton fraction went up from 75% to 85% when the rf power increased from 1400 to 1800 W.

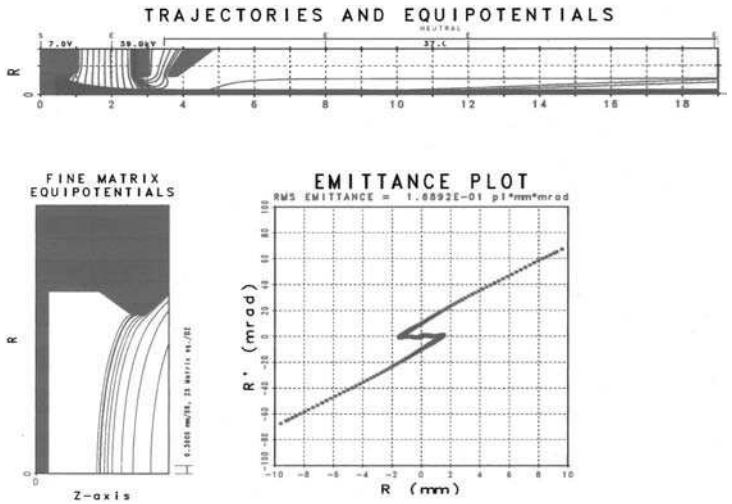

FIG. 6. (Top) PBGUNS simulation of the 35 keV, 44 mA positive hydrogen beam with 80% proton fraction (35 mA). (Bottom) plasma meniscus and the beam emittance pattern at 19 cm downstream from the plasma electrode. Over 98% of the beam is contained in the parallel, 3.8-mm-diameter beam core. The extraction aperture was 11.4 mm in diameter and the extraction gap was 17 mm.

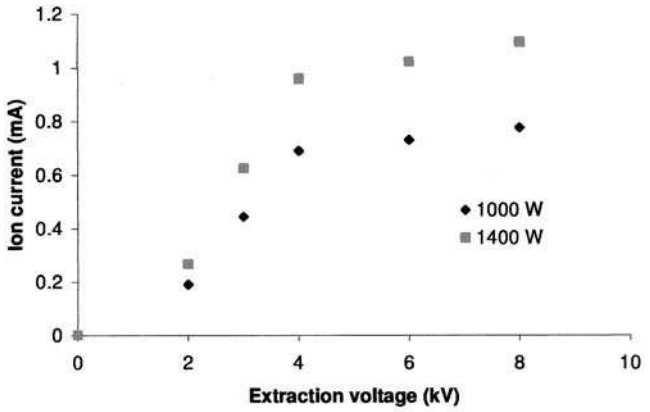

FIG. 8. Measured total ion current as a function of the extraction voltage at 1000 W and 1400 W of rf power and 20 mTorr source pressure.

This result met the goal set for the proton fraction.

The source operated optimally around 20 mTorr pressure. When the pressure was reduced, the matching conditions changed and the transformer turn ratio had to be adjusted. This prevented reliable comparison of source performance at different source pressures, and the source operation was optimized for pressures around 20 mTorr. During testing in Berkeley, the source operated reliably for hours at a time.

IV. PLASMA PROBE MEASUREMENTS

A commercially available rf compensated Langmuir probe system was used to make measurements of axial profiles of ion density, electron temperature, and plasma potential. A SmartProbe™ with auto-linear drive mechanism from Scientific Systems[9] was mounted on the laser inlet port of the source.

The probe tip was a 0.2-mm-radius tungsten wire of 1 mm length. The data were analyzed with the SmartProbe software (SMARTSOFT™, Version 3.31). The software determined the plasma potential by approximating the ''knee'' of the probe characteristic as the intersection of lines fit to the regions of electron collection and electron saturation. As an estimate of the error in the analysis of the probe characteristics, the data were also fit for the best agreement in the ion saturation and electron collection regions of the probe characteristic only. The plasma potential was calculated both directly from the fits, and by using the floating potential and electron temperature, as $V_p = V_f + 3.3T_e$. The error bars in Fig. 11 (one shown per trace) represent the largest discrepancy between the calculations, and those in Fig. 12 represent the standard deviation of the values obtained from the various methods of calculating plasma potential. They do not account for systematic error, which is not known, or for variation in measured probe characteristics at the same plasma conditions, which was seen to be considerably smaller. Probe scans were taken as plasma conditions varied with neutral gas pressure and rf power. Measured values and trends for the plasma parameters were consistent with those calculated from a cylindrical discharge model, in which the plasma itself is considered to be contained within a cylindrical volume of uniform bulk plasma parameters, including density, electron temperature, and plasma potential.[10]

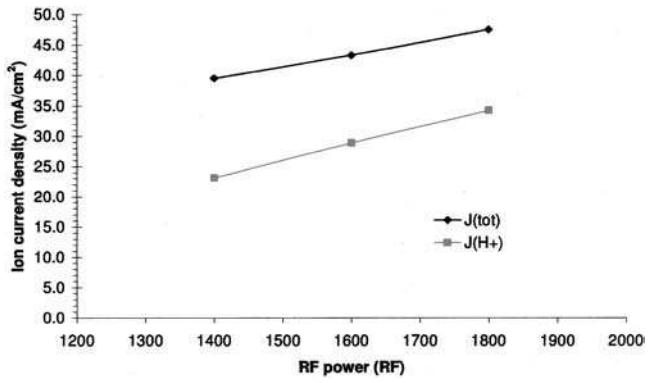

FIG. 9. The measured proton and total ion current densities as a function of rf power at 20 mTorr source pressure.

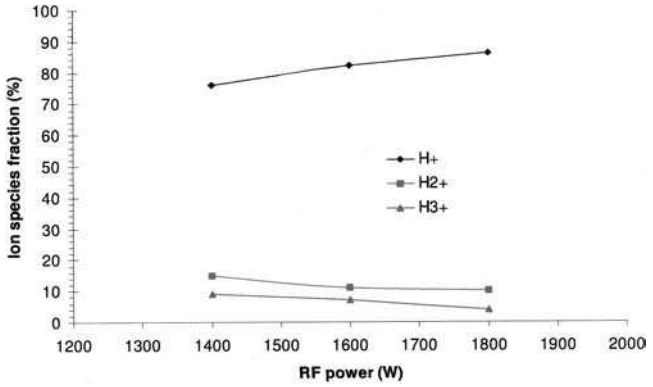

FIG. 10. Hydrogen species fraction as a function of rf power at 20 mTorr source pressure.

The ion density (n_i) increased with both rf power and neutral gas pressure, as would be expected. The maximum ion density measured was $2\times10^{12}\,\mathrm{cm}^{-3}$, at 1400 W input power and 30 mTorr source pressure, with values of $n_i \approx 10^{11}\,\mathrm{cm}^{-3}$, more typical for operation at 1000 W input power and 12 mTorr. These values are calculated using the

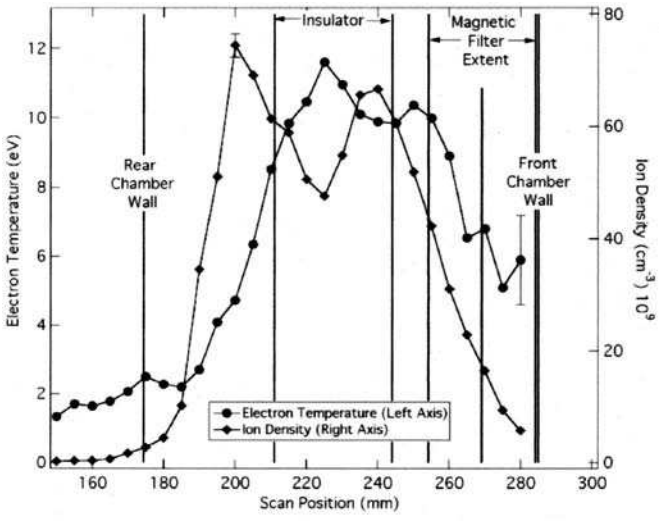

FIG. 11. Axial variation of electron temperature and ion density in source with 1000 W rf power and 12 mTorr source pressure.

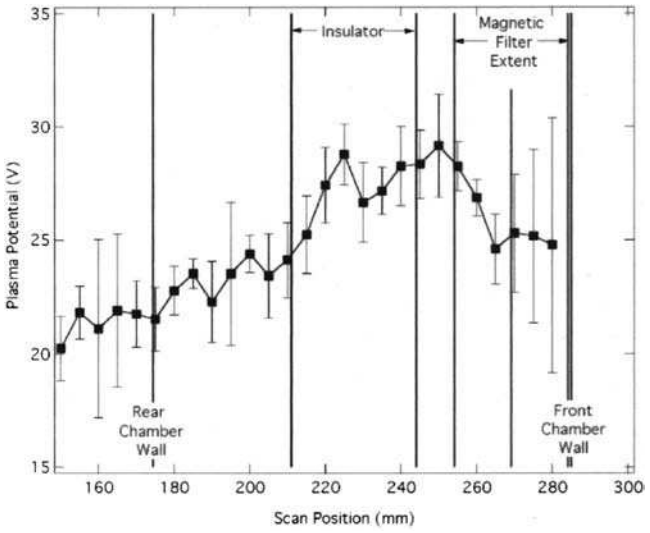

FIG. 12. Axial variation of the plasma potential at 1000 W rf power and 12 mTorr source pressure.

proton mass of 1 amu, and would be higher if the actual effective mass, including molecular ions and impurities, were used instead. Both the plasma potential and the electron temperature dropped with increasing pressure, and stayed constant as the rf power varied, as expected. Figure 11 shows the axial profile of the measured ion density and electron temperature in the source.

The motional Stark effect diagnostic for which the source will be used is very sensitive to the axial energy spread of the final neutral beam. Laser-induced fluorescence measurements will be performed on the beam, with the laser wavelength matched to the Doppler-shifted Hα spectral line. Any axial energy spread in the beam will result in broadening of the Doppler-shifted line, and is undesirable. Previous work has correlated axial energy spread with variation in plasma potential in the neutral-beam source,[4] making the measurement of the variation of plasma potential in the source of particular interest. Figure 12 plots the measured axial plasma potential distribution in the source. The variation of plasma potential is seen to be on the order of $\sim$5 eV. This is comparable to the lowest energy spreads reported in rf sources, on the order of 3 eV.[6] Factors such as rf coupling and accelerating power supply ripple may also contribute to the beam's axial energy spread.

ACKNOWLEDGMENTS

This work is supported by Nova Photonics, Inc. under U.S. Department of Energy Grant DE-FG02-01ER54616 and by the U.S. Department of Energy under Contract No. DE-AC03-76SF00098. One of the authors (S.K.H.) would like to thank the Finnish Academy of Science and Letters for additional support. Another (E.L.F.) gratefully acknowledges the support of a Hertz Foundation Graduate Fellowship. The authors would also like to thank P. Efthimion for the loan of equipment and for valuable discussions.

[1] K. W. Ehlers and K. N. Leung, Rev. Sci. Instrum. **54**, 1296 (1983).
[2] D. Wutte, S. Freedman, R. Gough, Y. Lee, M. Leitner, K. N. Leung, C. Lyneis, D. S. Pickard, M. D. Williams, and Z. Q. Xie, Nucl. Instrum. Methods Phys. Res. B **142**, 409 (1998).
[3] F. M. Levinton, Rev. Sci. Instrum. **70**, 810 (1999).
[4] Y. Lee, R. A. Gough, W. B. Kunkel, K. N. Leung, and L. T. Perkins, Nucl. Instrum. Methods Phys. Res. A **374**, 1 (1996).
[5] K. W. Ehlers and K. N. Leung, Rev. Sci. Instrum. **52**, 1452 (1981).
[6] Y. Lee, R. A. Gough, W. B. Kunkel, K. N. Leung, L. T. Perkins, D. S. Pickard, L. Sun, J. Vujic, M. D. Williams, and D. Wutte, Rev. Sci. Instrum. **68**, 1398 (1997).
[7] J. E. Boers, *Proc. of the 1995 Particle Accelerator Conference*, 1995, p. 2312.
[8] S. K. Hahto, S. T. Hahto, J. W. Kwan, K. N. Leung, and L. R. Grisham, Rev. Sci. Instrum. **74**, 2987 (2003).
[9] Scientific Systems Ltd., Unit 3, Howth Junction Business Park, Kilbarrack, Dublin 5, Ireland; SmartProbe Automatic Langmuir Probe User Manual, 2002; [info@scisys.com], [www.scisys.com].
[10] M. A. Lieberman and A. J. Lichtenberg, *Principles of Plasma Discharges and Materials Processing* (Wiley, New York, 1994), pp. 56–57.